

Electronic Supplementary Information

Correlation between the structural characteristics, oxygen storage capacities and catalytic activities of dual-phase Zn-modified ceria nanocrystals

Fangjian Lin,^{ab} Renaud Delmelle,^c Thallada Vinodkumar,^d Benjaram M. Reddy,^d
Alexander Wokaun^{*b} and Ivo Alxneit^{*ab}

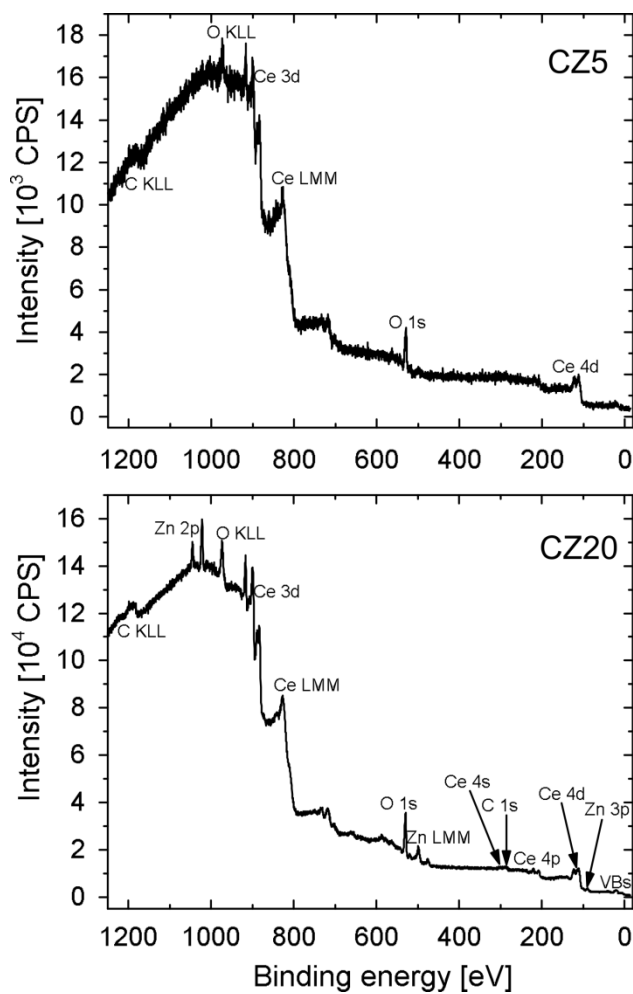


Figure S1. XPS survey spectra of CZ5 (top) and CZ20 (bottom).

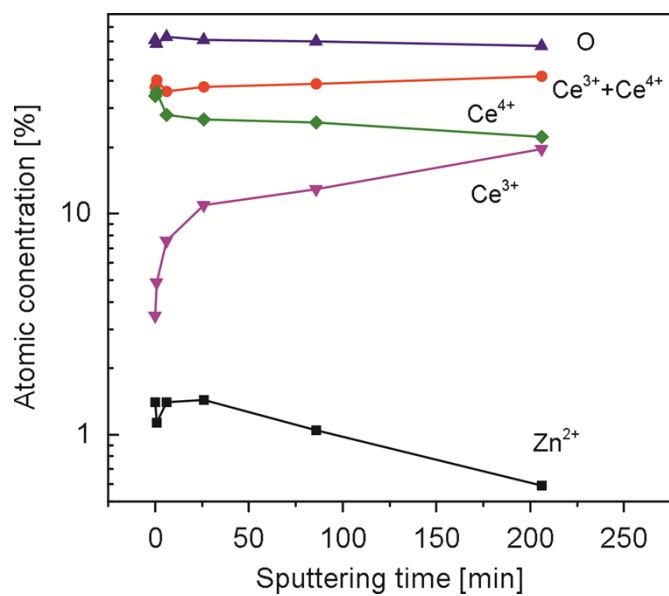


Figure S2. Depth profiles of O, Ce, and Zn of sample CZ5 over the course of ~3 h sputtering.

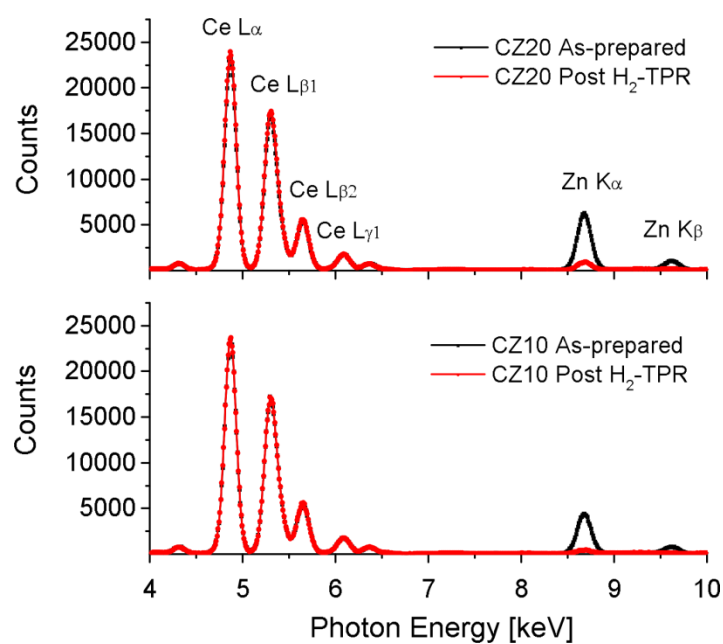


Figure S3. XRF spectra of CZ20 (top) and CZ10 (bottom) samples as-prepared and after H₂-TPR.

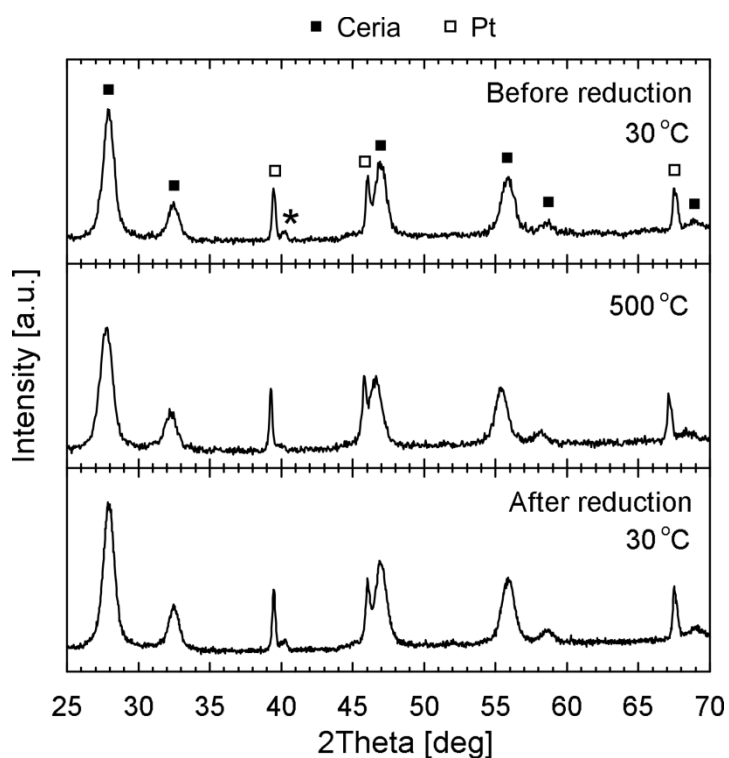


Figure S4. *In situ* XRD patterns of CZ20 under 10% H₂ in N₂ at 30 °C (top, before reduction), at 500 °C (middle), and at 30 °C (bottom, after reduction). No peaks attributed to ZnO or Zn is observed. The peaks marked by the asterisk could be due to that the Pt substrate is not flat (i.e. not on the same height).

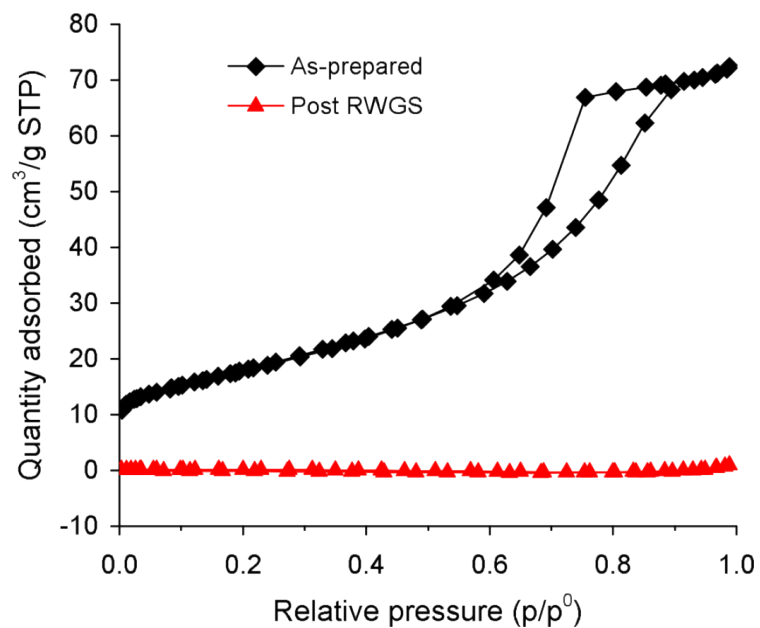


Figure S5. N₂ adsorption-desorption isotherms of pure ceria as prepared (black, diamond) and after the RWGS reaction (red, triangle).

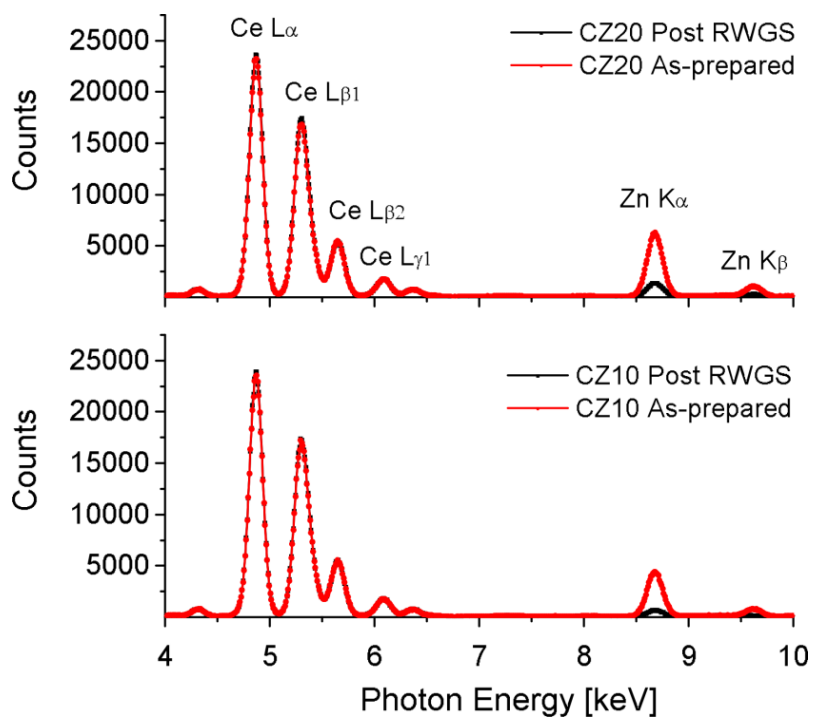


Figure S6. XRF spectra of CZ20 (top) and CZ10 (bottom) samples as-prepared and after the RWGS reaction (Figure 10).

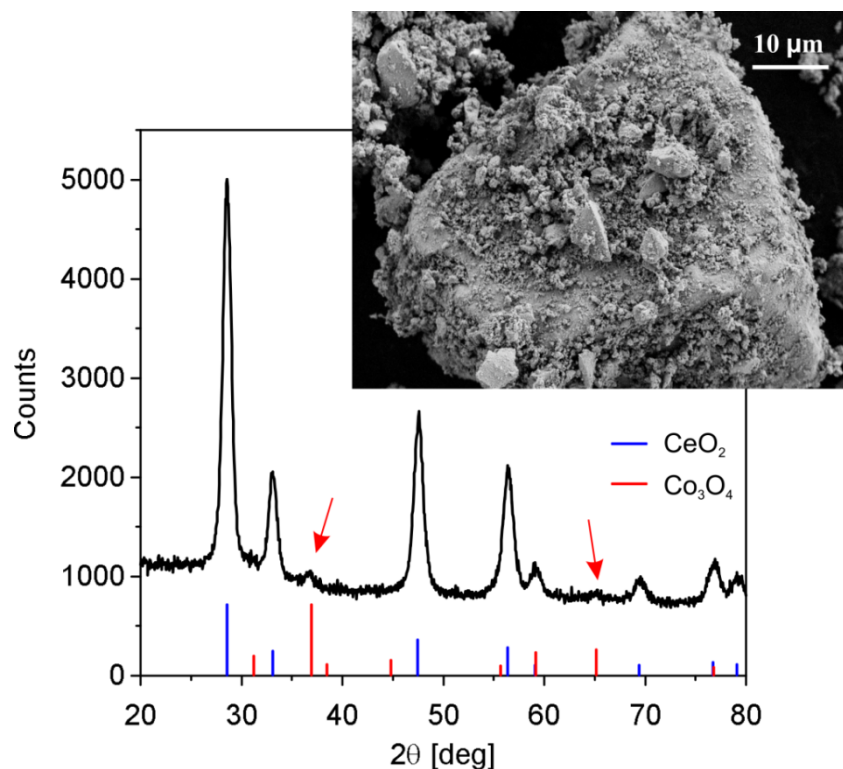


Figure S7. SEM image and XRD pattern of 10 mol% CoO_x impregnated on CZ10, confirming dispersion and poor crystallinity of cobalt oxide on CZ10 particles. The SEM image was recorded with a Zeiss Supra VP55 high resolution field emission scanning electron microscope at 3 kV.

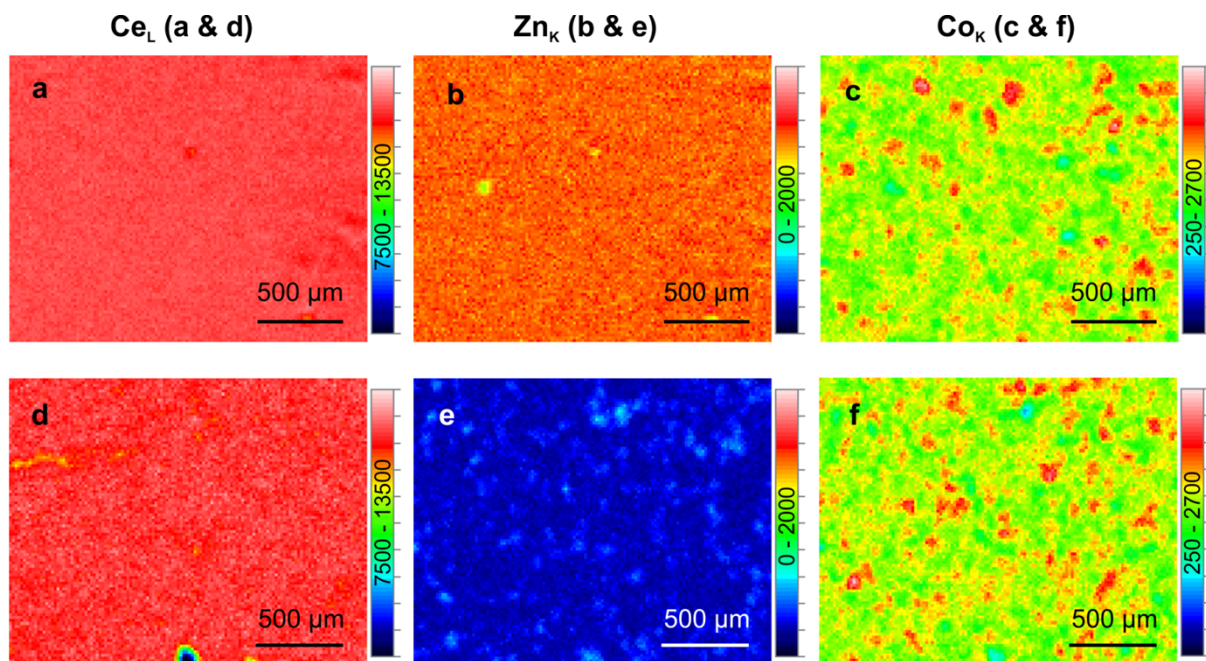


Figure S8. XRF elemental maps of $\text{CoO}_x/\text{CZ10}$ as-prepared (top row) and after RWGS reaction (bottom row): Ce_L (a & d) showing no obvious changes in the cerium concentration and spatial distribution, Zn_K (b & e) showing significant loss of zinc, and Co_K (c & f) showing excellent thermal stability of cobalt dispersion. Note that the maps of identical element are plotted in the same color scale.